Available online at www.sciencedirect.com
SCIENCE DIRECT
Journal of Catalysis 234 (2005) 431–437
JOURNAL OF CATALYSIS
www.elsevier.com/locate/jcat

Immobilization of iron(III) porphyrins on exfoliated Mg–Al layered double hydroxide, grafted with (3-aminopropyl)triethoxysilane

Fernando Wypych *, Alesandro Bail, Matilte Halma, Shirley Nakagaki

Centro de Pesquisas em Química Aplicada (CEPESQ) and Laboratório de Bioinorgânica e Catálise, Departamento de Química, Universidade Federal do Paraná (UFPR), CP 19081, 81531-990, Curitiba, PR, Brazil

Received 6 May 2005; revised 7 July 2005; accepted 12 July 2005

Abstract

Mg–Al layered double hydroxide (LDH) intercalated with dodecylsulfate, was exfoliated in toluene, and the single-layer suspension was reacted with (3-aminopropyl)triethoxysilane (3APTS) in the same solvent. After washing with toluene and acetone to remove the excess reagent and drying procedure, the solid was reacted with neutral and anionic iron(III) porphyrins in toluene and methanol, respectively. The products were analyzed by powder X-ray diffraction, Fourier transform infrared spectroscopy, electron paramagnetic resonance, ultraviolet–visible light, and atomic absorption spectrometric techniques. All of the data are consistent with the grafting of the LDH interlayers with 3APTS and immobilization of the iron porphyrins on the pendent terminal amino groups positioned at the top the grafted molecule. Based on these results, a schematic representation for the immobilization and preliminary catalytic oxidation reactions is presented.

Keywords: Layered double hydroxides; Exfoliation; Porphyrin; Grafting; Immobilization; Catalysis; Oxidation

1. Introduction

Layered materials belong to a special class of compounds in which the crystals are built by stacking "two-dimensional" units known as layers that are bound to each other through weak forces [1,2]. Intercalation reactions occur by the topotactic insertion of mobile guest species (neutral molecules, anhydrous or solvated ions) into the accessible crystallographic-defined vacant sites located between the layers (interlayer spacing) in the layered host structure. In these intercalation compounds, strong covalent bonds occur in the layers and weak interactions occur between host lattice and guest species or co-intercalated solvents. Ionic and solvent exchange reactions are related to the replacement of solvated guest species (ions) placed into the interlayer spacing. In this case, only the solvent, the anhydrous ions, or the solvated ions can be replaced, depending on the reaction conditions.

Exfoliation reactions involve the separation of individual layers in an appropriate solvent. Literally, this reaction is a process of rupture of a layered crystal in such a way that stacked single layers are removed from the crystal and taken to suspension. Investigation of the exfoliation of layered compounds started with transition metal dichalcogenides, specially molybdenum disulfide, in the 1980s [3–5].

This process of separation of individual layers potentially could be used for reactions of direct functionalization (grafting), because in those conditions there are no bonds among the layers, which can hinder the access of the reactants to the interlayer spacing. Grafting reactions occur by establishing covalent bonds between the reactive groups of the layer and an adequate reactant molecule, which ensures greater chemical, structural, and thermal stability for the compound. These reactions can be restricted to the crystal surface (in which case the basal spacing remains unchanged) or the layer surface (in which case an interlayer expansion occurs, if the single layers are restacked). These compounds can be collectively defined as "hybrid" materials or, more specifically, surface-modified inorganic layered materials.

* Corresponding author. Fax: +55-41-3361-3186.
E-mail address: wypych@quimica.ufpr.br (F. Wypych).

0021-9517/$ – see front matter
doi:10.1016/j.jcat.2005.07.013

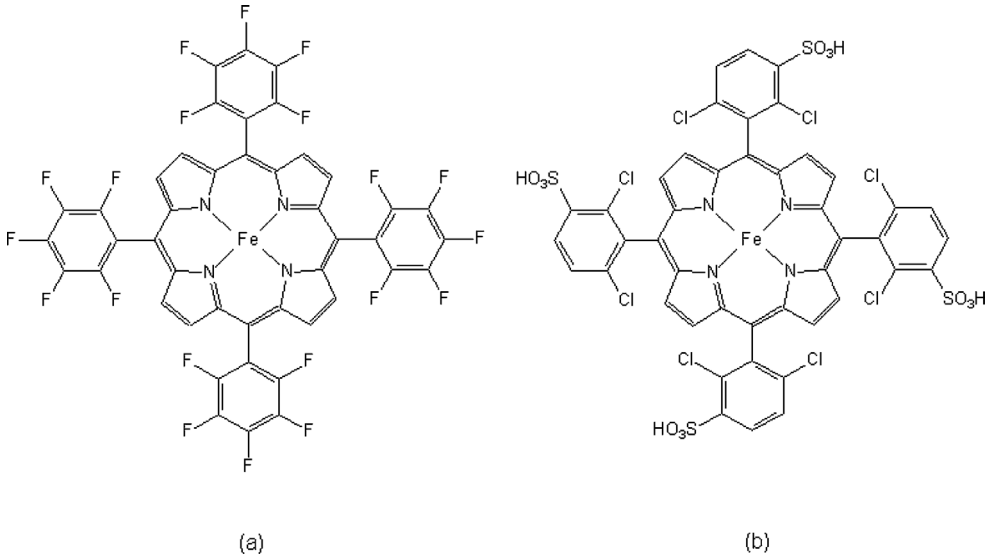

Fig. 1. Molecular structure of the iron(III) porphyrin used in this work. (a) Fe(TPFPP); (b) Fe(TDCSPP).

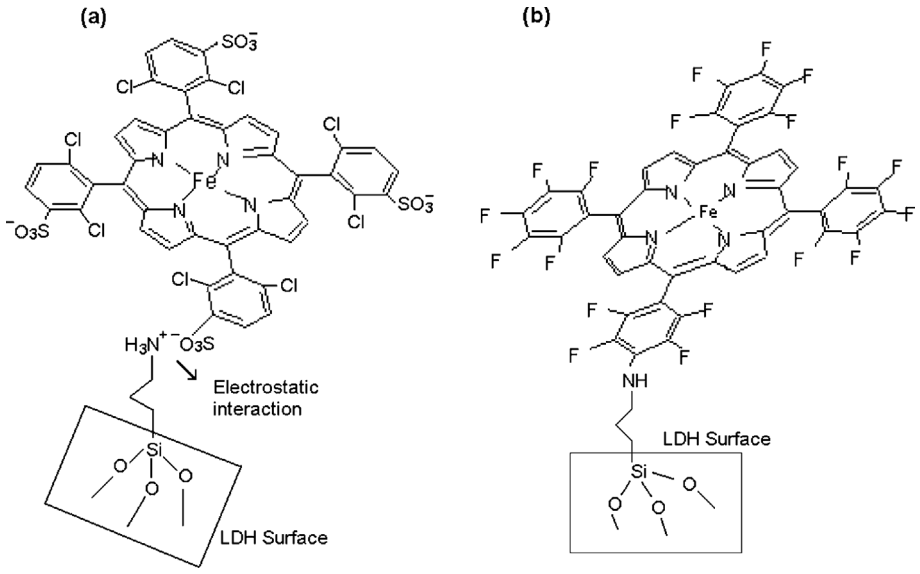

Fig. 2. Schematic representation of the (a) anionic iron(III) porphyrin (Fe(TDCSPP)) immobilized after protonation the terminal amino group in methanol solution [16] and (b) immobilization of the neutral iron(III) porphyrin (Fe(TPFPP)) by covalent bonding between the iron(III) porphyrin *para*-fluorine from the *meso*-pentafluorophenyl ring substituents and the amino terminal groups from the 3APTS [21–24].

Layered double hydroxides (LDHs) have the generic formula $[M_{1-x}{}^{2+}M_x{}^{3+}(OH)_2]^{x+}(A^{m-})_{x/m} \cdot nH_2O$, where M^{3+} and M^{2+} represent metal ions in octahedral sites and A^{m-} represents the interlayer anion. In these compounds, the trivalent metal isomorphically substitutes a metal in the divalent state of oxidation of the hydroxide structure, generating charges that are compensated for by the intercalation of hydrated anions [6–8]. Recently the process of exfoliation has also been developed for LDH, using different procedures [9–12], and our research groups have proposed the process of exfoliation of LDH and grafting of the single layers with silanes and phosphonates [13]. More recently, the reaction of exfoliated LDH with a silane was confirmed experimentally [14].

Based on the exfoliation and possibility of grafting the LDH single layers to produce alternative supports for immobilization of catalysts, the objective of this paper is to describe the process of exfoliation of Mg–Al-LDH intercalated with dodecylsulfate in toluene, functionalization with (3-aminopropyl)triethoxysilane (3APTS) and immobilization of iron(III) porphyrins (Figs. 1 and 2).

2. Experimental

The neutral iron(III) porphyrin Fe(TPFPP)Cl (5,10,15, 20-tetrakis(pentafluorophenyl)-1*H*, 23*H*-porphine iron(III)

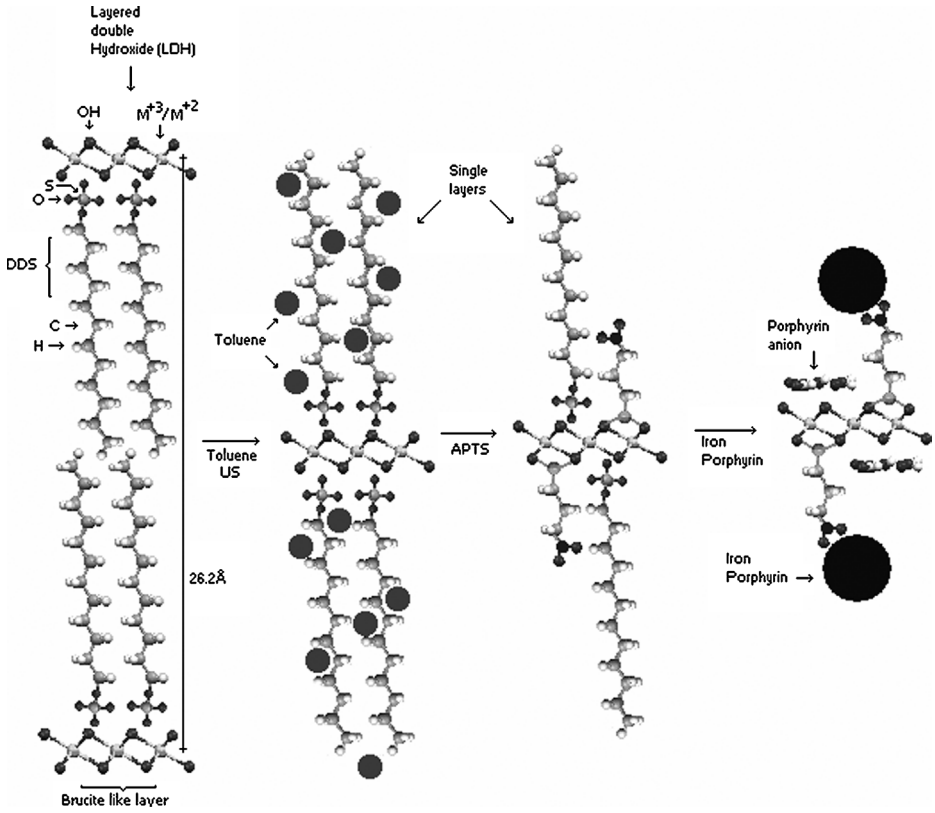

Fig. 3. Schematic representation of the exfoliation of Mg–Al-LDH in toluene, grafting with (3-aminopropyl)triethoxysilane (3APTS) and immobilization of the anionic iron porphyrin.

chloride) was purchased from Aldrich (Soret band at 414 nm and molar absortivity (ε) in toluene $= 8.9 \times 10^4$ L mol^{-1} cm^{-1}).

The anionic-charged iron(III) porphyrin Fe(TDCSPP) (5,10,15,20-tetrakis(dichlorophenyl)-21H, 23H-porphine-m', m'', m'''-tetrasulphonic acid iron(III) chloride) was synthesized and characterized as reported previously [15,16]. (Soret band at 412 nm molar absortivity (ε) in methanol $= 18 \times 10^3$ L mol^{-1} cm^{-1}.)

Mg–Al-LDH intercalated with dodecylsulfate was prepared as described previously [17]. Briefly, nitrate salts of aluminum and magnesium were added dropwise to a solution of sodium dodecylsulfate at pH = 10 under inert atmosphere. The white solid was washed five times with water, centrifuged at 3500 rpm, and dried at 50 °C for 24 h (LDH-DDS).

Exfoliation of the layered compound was performed as follows: 1.0 g of the Mg–Al-LDH was added to a three-neck reaction flask containing 250 mL of toluene, and the mixture was subjected to an ultrasound bath for 4.5 h at room temperature (ca. 21 °C). After the suspension was kept for about 30 min, an extremely fine white and voluminous gel formed at the bottom of the reactive flask.

The white gel was reacted with ca. 15 times the stoichiometric amount of (3-aminopropyl)triethoxysilane (3APTS), with the reaction conducted under argon atmosphere for 5 h at 60 °C. The precipitated solid was isolated by centrifugation, washed three times with toluene and three times with acetone, with each step followed by suspending the solid, then centrifugation. Finally, the white solid was dried in vacuum for 12 h (LDH-DDS-APTS).

The process of neutral iron(III) porphyrin immobilization was conducted by dispersing the grafted solid (50 mg) in 10 mL of toluene, containing 1.8×10^{-6} mol of Fe(TPFPP)-Cl. The suspension was refluxed and stirred for 22 h under argon until the color of the solution was removed, which occurred after 12 h. The solid was washed with toluene and dried at 60 °C for 24 h. To determine quantitatively the amount of the iron porphyrin still present in the solution, and thus the amount present in the solid, all of the washing solutions were collected and analyzed by ultraviolet–visible (UV–vis) light spectroscopy. The general procedure for the immobilization of anionic-charged iron porphyrin Fe(TDCSPP) was similar to that used for the immobilization of Fe(TPFPP), but with the solvent replaced by methanol.

Fig. 3 shows a schematic representation of the exfoliation, grafting, and immobilization of the iron porphyrin.

Powder X-ray diffraction (PXRD) analysis was done with the solid material placed on a glass sample holder and spread out to form a thin layer. A Shimadzu XRD-6000 diffractometer was used with Cu-K$_\alpha$ radiation ($\lambda = 1.5418$ Å) with a dwell time of 1° min^{-1}, in the θ–2θ Bragg–Brentano geometry. All measurements were made using a generator voltage of 40 kV and an emission current of 30 mA.

Fourier transform infrared (FTIR) spectroscopy was done using a Biorad FTS 35000GX spectrophotometer with special KBr discs prepared after mixing (1%) each of the test samples with dry KBr. Analyses were performed in transmission modes of 400–4000 cm^{-1}, with a resolution of 2 cm^{-1} and accumulation of 16 scans.

Electron paramagnetic resonance (EPR) measurements of the powder materials were made with a Bruker ESP 300E spectrometer at X-band (ca. 9.5 GHz) at 293 or 77 K using liquid N_2.

Absorption atomic spectroscopy (AAS) was performed using a Shimadzu AA6800 spectrophotometer coupled to an ASC 6100 autosampler (graphite tube). The experiments were performed under argon atmosphere, and a Fe cathode lamp was operated at 248.3 nm with a 0.5-nm spectral bandpass. Deionixed water produced by a Milli-Q (18 mΩ) system was used for the preparation of all solutions. The iron standard solutions were prepared by diluting the 1.000-mg L^{-1} stock solution (Merck). Sample solutions were prepared by digesting 3.5 mg of the samples in 50% (v/v) HNO_3 for 30 min.

UV–vis measurements were performed in a Hewlett Packard-8452 A diode array spectrophotometer.

Iodosylbenzene (PhIO) was prepared as described previously [18,19]. It was obtained through the hydrolysis of iodosylbenzenediacetate following the methods described by Saltzmann and Sharefkin [18]. The purity was measured by an iodometric assay.

A typical catalytic oxidation reaction was carried out in a 2-mL thermostatic glass reactor equipped with a magnetic stirrer inside a dark chamber [15,16]. In a standard experiment within the reactor, solid catalyst and iodosylbenzene (FePor:PhIO molar ratio 1:10) were suspended in 0.350 mL of solvent (dichloromethane-acetonitrile, 1:1 mixture v/v) and degassed with argon for 10 min. The substrate (cyclohexane, FePor:substrate, molar ratio = 1:1000) was added and the oxidation reaction was done for 1 h under magnetic stirring. To eliminate any excess iodosylbenzene, sodium sulfite was added, and the products of the reaction were separated from the solid catalyst by exhaustive washing and centrifugation of the solid with an acetonitrile–dichloromethane mixture. The extracted solution was analyzed by capillary gas chromatography, and the amounts of the products were determined by the internal standard method. No products were detected when the catalyst was exfoliated or grafted LDH or in solutions set up without catalyst. Products from catalytic oxidation reactions were identified using a Shimadzu CG-14B gas chromatograph (equipped with a flame ionization detector) with a DB-WAX capillary column (J&W Scientific). After the first catalytic run for each catalyst solid, the supported catalysts were recovered from the solution reaction by filtration, washed thoroughly in Soxhlet extractor with different solvents, and finally dried for reuse. Reuse experiments are under progress.

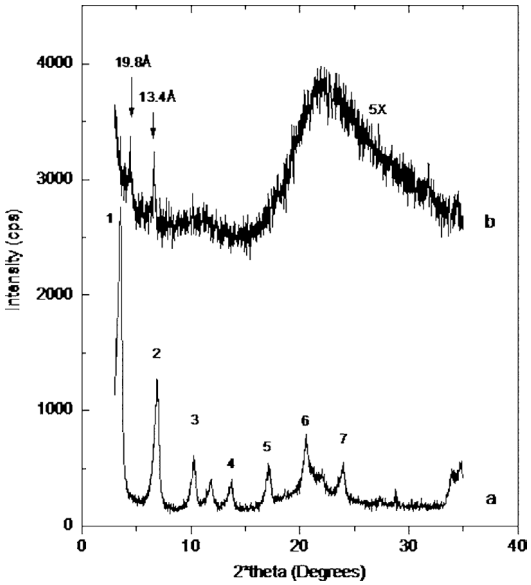

Fig. 4. Powder X-ray diffraction patterns of the LDH-DDS (a), after exfoliation and grafting with (3-aminopropyl)triethoxysilane (LDH-DDS-3APTS) (b). The numbers represent the basal reflections sequence (1, 25.8; 2, 12.92; 3, 8.62; 4, 6.49; 5, 5.18; 6, 4.34; and 7, 3.74 Å).

3. Results and discussion

The concentration of iron porphyrins in the grafted LDH support at the end of the immobilization process was confirmed by quantification of the iron porphyrins in the reaction solutions and all extracts obtained in the washing procedures (by UV–vis spectroscopy) or by analysis of iron content by AAS. The UV–vis analysis yielded 1.8×10^{-5} mol of Fe(TDCSPP)/g LDH (84%) and 7.6×10^{-6} mol of Fe(TPFPP)/g LDH (28%); the AAS analysis yielded slightly lower concentrations of both iron porphyrins in the support.

Fig. 4 shows the XRD pattern of the products obtained as shown schematically in Fig. 3. As this figure shows, LDH-DDS (Fig. 4a) presents several basal peaks with a basal distance of 26.2 Å, matching the value reported in the literature [17,20]. After exfoliation and grafting of 3APTS (Fig. 4b), the material restacks poorly, and only two discrete diffraction peaks and a broad amorphous band are observed. Because the size of the grafted 3APTS is 7.5 Å in size [14] and the LDH layer is ca. 4.8 Å thick, the observed diffraction peak at 19.8 Å is related to the grafting of the 3APTS to both sides of the layers and restacking in a double-layer arrangement. The peak at 13.4 Å can be attributed to the restacking of the layers in a monolayer arrangement. When the iron porphyrin is immobilized on the grafted layers, the XRD pattern shows an amorphous profile (not shown). Because the layers are poorly restacked, making the terminal amino groups available, this material is an adequate matrix for the immobilization of catalysts. Metals such as copper, which can be easily coordinated by the amino terminal group, can also be potentially removed from solutions and retained by the solid. The two proposed alternatives for the immobilization of the

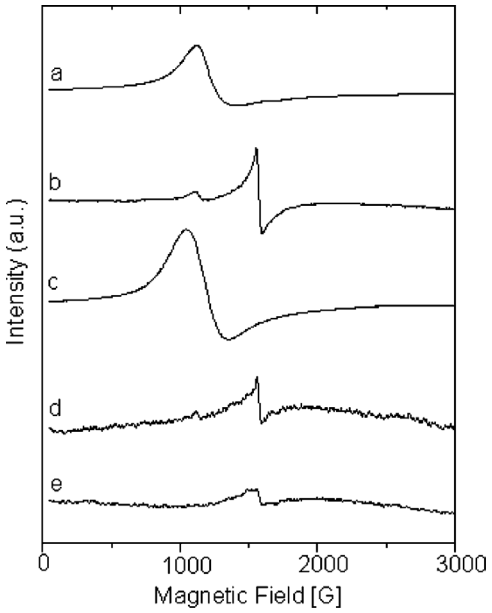

Fig. 5. EPR spectra obtained for the solids: (a) Fe(TDCSPP) at room temperature, (b) Fe(TDCSPP)/LDH-3APTS at 77 K, (c) Fe(TPFPP) at 77 K, (d) Fe(TPFPP)/LDH-3APTS at 77 K and (e) LDH-3APTS at 77 K.

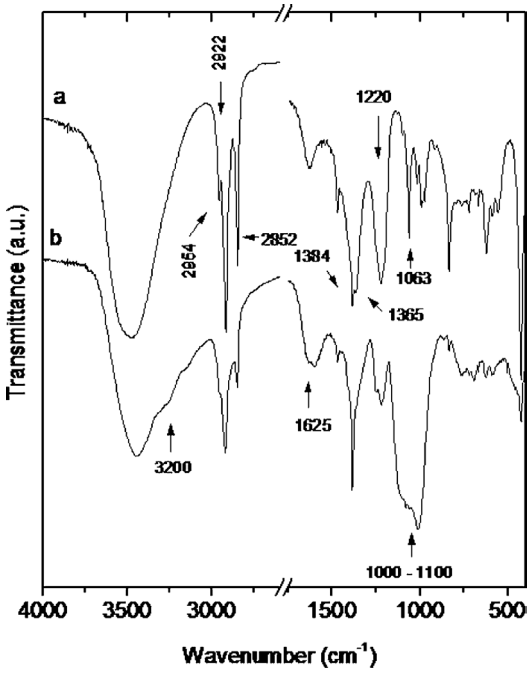

Fig. 6. FTIR spectra obtained for the solids (a) LDH-DDS and (b) LDH-DDS-3APTS.

anionic and neutral iron porphyrin are schematically illustrated in Fig. 2.

Protonation of the amino terminal groups from 3APTS provides a positive charge for the interaction of the anionic groups from the iron porphyrin Fe(TDCSPP) (Fig. 2a) [16]. This immobilization mechanism is not possible for the neutral Fe(TPFPP). Covalent bonding is an alternative approach for this immobilization, because the neutral iron porphyrin presents the pentafluorophenyl groups at the *meso*-positioned porphyrin ring, which can be bonded to the functionalized silica by nucleophilic aromatic substitution. This mechanism is explained by the reaction of fluorine atoms from the meso porphyrin groups and pendant amino groups from the grafted molecule [21–23]. The excess amine groups from the 3APTS at the surface could also lead to the formation of some mono or double coordination to the iron(III) from the neutral or charged iron(III) porphyrin [23]. The formation of penta-coordinated species in sufficient amounts could be detected by qualitative EPR analysis, because mono amino iron(III) porphyrin is known as a low-spin iron(III) porphyrin and present a typical EPR signal around $g = 2.0$ [23,24]. But on the other hand, it is well known that amino double bonded to iron(III) porphyrin (hexa-coordinated), particularly those with electron-withdrawing substituents such as Fe(TPFPP) or Fe(TDCSPP) [22], can reduce the iron(III) to iron(II) species, which are EPR-silent. Detecting small amounts of amino-coordinated species in the sample is very difficult in a qualitative EPR analysis.

EPR spectra of the solid anionic iron porphyrin Fe(TDCSPP) (Fig. 5a) and the solid neutral iron porphyrin Fe(TPFPP) (Fig. 5c) show signals with $g = 6.0$ typical of the iron(III) porphyrin high-spin 5/2 complex [3]. The solid LDH-3APTS is EPR-silent (Fig. 5e), showing slight contamination of high-spin Fe(III) in rhombic symmetry (at about 1500 G). The presence of the typical Fe(III) rhombic EPR signal with $g = 4.3$ (Fig. 5, b and d) confirms that the iron(III) porphyrin is immobilized in the support, being distorted from the axial symmetry ($g = 6.0$) and high rhombicity ($g = 4.3$). A chlorine ion as a penta-coordinated ligand is likely present, instead of amino groups, from the surface groups of the support. EPR also confirms that no demetallation process occurred during the immobilization procedure [25,26].

In addition, the UV–vis spectrum of the resulting material (in nujol mull) after immobilization of the neutral Fe(TPFPP) shows the Soret band at 418 nm (not shown). In double-bonded amino Fe(II) porphyrin complex formation, a large red shift of the Soret band would be expected [22]. This result suggests that the neutral iron(III) porphyrin is preferentially immobilized at the surface of the grafted LDH, although the possible presence of some penta- or hexa-coordinated amino species in small amounts cannot be excluded.

The presence of the iron(III) porphyrins with similar behavior when metalloporphyrins were immobilized in LDH by different processes has been observed previously [7,15, 27].

Fig. 6 shows the FTIR spectra of LDH-DDS (a) and LDH-3APTS (b). Fig. 6a shows the characteristic DDS bands [16], particularly the bands at 2954, 2922, and 2852 cm^{-1}, attributed to C–H stretching bonds of the organic skeleton and at 1220 and 1063 cm^{-1}, attributed to the sulfate group. Extra bands were also observed at 1384 and 1365 cm^{-1}, attributed to nitrate and carbonate ions, respectively, co-intercalated with DDS. The presence of nitrate is

explained by the precipitation of the respective aluminum and magnesium nitrate and carbonate from the atmospheric carbon dioxide.

After the grafting reaction, the bands of sulfate and carbonate were reduced in intensity and new bands in the region of 1000–1100 cm^{-1}, attributed to silicon bonded to different atoms, were introduced. The nitrate band remains in the grafted derivative. New broad bands related to the N–H bonds are present in the regions of 3200 and 1625 cm^{-1}, confirming the grafting reaction.

4. Preliminary catalytic studies

Two iron porphyrins are supported on LDH-3APTS by exfoliation and functionalization. The obtained catalysts contain 1.8×10^{-5} mol of Fe(TDCSPP)/g LDH (84%) and 7.6×10^{-6} mol of Fe(TPFPP)/g LDH (28%) and are not released from the support after washing with different organic solvents, as would be expected for the iron(III) porphyrin bearing four negative charges [Fe(TDCSPP)] [15] and the neutral iron(III) porphyrin Fe(TPFPP) if covalent bonds are formed. Initially, coordinative binding of the neutral iron(III) porphyrin to the amino groups from the support seems to provide a simple route for immobilization. However, the inherent weakness of the ligand–iron bond that could cause leaching of the catalyst does not agree with the experimental observations for the neutral iron(III) porphyrin. The resistance of the anionic iron(III) porphyrin to the washing process suggests that the neutral iron(III) porphyrin is tightly attached to the support [22]. The resistance of both iron(III) porphyrins to the washing process can facilitate the future reuse of the solid catalysts.

The catalytic activity of the both iron porphyrin-supported catalysts, (Fe(TDCSPP)/LDH-3APTS and Fe(TPFPP)/LDH-3APTS), were investigated on the oxidation of weakly reactive alkanes such as cyclohexane. Preliminary results are given in Table 1.

The catalytic conversion of cyclohexane to cyclohexanol is observed for both immobilized catalysts. The increase of the alcohol yield is accompanied by an increase in ketone, suggesting that the immobilized iron porphyrins have poor selectivity to alcohol.

Recently it was observed that iron porphyrin Fe(TDFSPP) (5,10,15,20-tetrakis(difluorophenyl)-21H,23H-porphine-m,m',m'',m'''-tetrasulfonic acid iron(III) chloride), a porphyrin structurally similar to Fe(TDCSPP), immobilized at the LDH surface (containing interlayer carbonate anions that are difficult to exchange) with a high conversion of cyclohexane to cyclohexanol (90%) and high selectivity to alcohol (alcohol:ketone % ratio = 16) [27]. These results were explained by the easy access of the PhIO and the substrate to the catalytic iron site resulting from the immobilization of Fe(TDFSPP) mainly at the surface of the LDH crystals. The results in Table 1 for the iron porphyrins Fe(TDCSPP) and Fe(TPFPP) immobilized on LDH-3APTS, although different from the results previously reported for Fe(TDFSPP), show modest catalytic conversion with low selectivity of the substrate to alcohol.

Table 1
Results of cyclohexane oxidation reactions—iodosylbenzene catalyzed by metalloporphyrins before and after immobilized on grafted LDH[a]

Run	Complex[b]	Cyclohexane	
		Alcohol yield[b] (%)	Ketone yield[c] (%)
1	Fe(TDCSPP)/LDH-3APTS	11	22
2	Fe(TPFPP)/LDH-3APTS	36	57
3	Fe(TPFPP)	85	6
4	Fe(TDCSPP)	8.2	3.4
5	LDH	<5	–

[a] Conditions: purged with argon during 10 min; substrates: cyclohexane, solvent: dichloromethane/acetonitrile mixture (1:1 v/v); at room temperature.
[b] Iron complexes:PhIO:substrate molar ratio (mol:mol:mol ≅ 1:20:1000).
[c] Yields based on starting oxidant; 1 h of reaction. Control experiments yield <5% under all conditions.

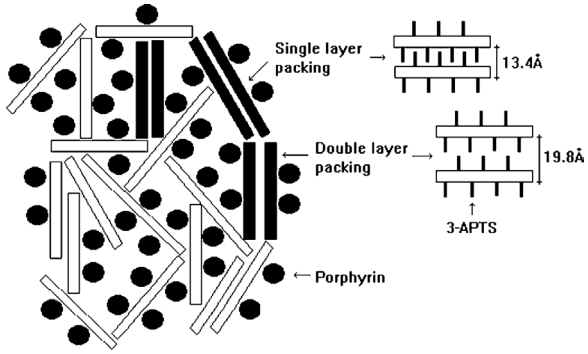

Fig. 7. Schematic representation of the catalysts FePor/LDH-3APTS.

To explain this behavior, a schematic representation of the catalyst is shown in Fig. 7. Because the iron(III) porphyrins are probably trapped inside the pores of the randomly stacked grafted LDH single layers, both iron(III) porphyrins are less accessible to the reagents to promote a high yield of products different from the Fe(TDFSPP), as reported previously [27]. But the alcohol produced by the catalytic conversion of cyclohexane remains close to the catalytic active sites and may be competing with cyclohexane, which will be further oxidized to ketone.

Recall that our XRD analysis (Fig. 4) revealed that most of the layers are unstacked, with a “house of cards” arrangement that generates pores of different sizes and morphologies. The EPR analysis (Fig. 5) showed a greater distortion of both of the iron porphyrins immobilized, indicating a similar coordination environment for both iron porphyrins with a greater distortion of the iron(III) sites.

Compared with the results obtained in heterogeneous catalysis, the homogeneous reaction for the Fe(TPFPP) (Table 1, run 3) demonstrated higher yield and greater selectivity to alcohol than Fe(TDCSPP) (run 4).

The solubility of the iron porphyrins Fe(TPFPP) (high) and Fe(TDCSPP) (low) in CH_2Cl_2:CH_3CN (1:1 volume ratio) solvent mixture in homogeneous catalysis certainly is an important factor in the yield of the iron porphyrin itself; see run 3 in Table 1, showing a high alcohol yield and high solubility of Fe(TPFPP).

The polar Fe(TDCSPP), poorly soluble in the solvent mixture, had a lower yield to alcohol than the heterogeneous systems. In this case, despite the low access of the reagents to the iron porphyrin catalytic active center as discussed earlier, the immobilization process slightly increases the catalytic activity of this iron(III) porphyrin.

The catalyst oxidative degradation in solution is often responsible for the low yield in catalytic reactions using metalloporphyrins [25]. In reactions using Fe(TDCSPP) or Fe(TPFPP), oxidative destruction is probably insufficient to cause the decrease in yield, because the two second-generation iron(III) porphyrins are known for their resistance to destructive oxidative conditions [28].

As shown in Table 1, under the same reaction conditions (heterogeneous catalysis), substantially better yields are obtained with immobilized iron porphyrin Fe(TPFPP)-LDH-3APTS than with Fe(TDCSPP)-LDH-3APTS. In homogeneous catalysis, the two *ortho*-chlorine substituents in each *meso*-phenyl porphyrin group in the Fe(TDCSPP) can avoid molecular interactions that can deactivate (by destruction of the iron porphyrin or dimerization). In contrast, after immobilization, the best catalytic results observed for Fe(TPFPP) were possibly due to the easy access of PhIO and substrate to the iron site, because of the small size of the five fluorine substituents compared with the *ortho*-chlorine substituent from Fe(TDCSPP) [15,27].

It is noteworthy that reactions using the LDH support itself without iron porphyrins (run 5, Table 1) gave very low hydroxylation yields (<5% of alcohol) under identical conditions, indicating that the catalytic effect in the hydroxylation of the cyclohexane can be attributed to the presence of iron porphyrin.

5. Conclusions

After exfoliation of a LDH and grafting of 3APTS to a single layer surface, two different iron(III) porphyrins were immobilized to the pendant organic molecule. Negative-charged iron(III) porphyrin [Fe(TDCSPP)] was immobilized in higher concentrations through electrostatic interaction ($–NH_3^+$ $^-O_3S–$), after protonation of the amine terminal groups. Most of neutral iron(III) porphyrin (Fe(TPFPP)) was probably immobilized through covalent bonds by nucleophilic aromatic substitution of fluorine atoms from the *meso*-pentafluorophenyl porphyrin substituents and amino groups from the grafted organic molecules. The catalytic behavior favors oxidation of cyclohexane, probably due to the high residence time of the substrate inside of the pores of the randomly stacked LDH single layers.

Acknowledgments

The authors acknowledge CNPq, CAPES, and PRONEX/MCT for financial support. They also thank Kestur Gundappa Satyanarayana for providing critical comments and helpful suggestions that improved the manuscript.

References

[1] R. Schöllhorn, in: W. MüllerWarmuth, R. Schöllhorn (Eds.), Progress in Intercalation Research, Kluwer Academic, Dordrecht, 1994.
[2] R. Schöllhorn, in: M.S. Whittingham, A.J. Jacobson (Eds.), Intercalation Chemistry, Academic Press, New York, 1982.
[3] P. Joensen, R.F. Frindt, S.R. Morrison, Mater. Res. Bull. 21 (1986) 457.
[4] P. Joensen, E.D. Crozier, N. Alberding, et al., J. Phys. C: Solid State Phys. 20 (1987) 4043.
[5] W.M.R. Divigalpitiya, R.F. Frindt, S.R. Morrison, Science 246 (1989) 369.
[6] J.L. Guimarães, R. Marangoni, L.P. Ramos, et al., J. Colloid Interface Sci. 227 (2000) 445.
[7] F. Wypych, G.A. Bubniak, M. Halma, S. Nakagaki, J. Colloid Interface Sci. 264 (2003) 203.
[8] F. Wypych, in: F. Wypych, K.G. Satyanarayana (Eds.), Clay Surfaces—Fundamentals and Applications, Academic Press, Amsterdam, 2004.
[9] M. Adachi-Pagano, C. Forano, J.P. Besse, J. Chem. Commun. 1 (2000) 91.
[10] T. Hibino, W. Jones, J. Mater. Chem. 11 (2001) 1321.
[11] G.A. Bubniak, W.H. Schreiner, N. Mattoso, F. Wypych, Langmuir 18 (2002) 5967.
[12] M. Jobbagy, A.E. Regazzoni, J. Colloid Interface Sci. 275 (2004) 345.
[13] F. Wypych, K.G. Satyanarayana, J. Colloid Interface Sci. 285 (2005) 532.
[14] A. Park, H. Kwon, A.J. Woo, S. Kim, Adv. Mater. 17 (2005) 160.
[15] S. Nakagaki, M. Halma, A. Bail, G.G.C. Arizaga, F. Wypych, J. Colloid Interface Sci. 281 (2004) 417.
[16] S. Nakagaki, F.L. Benedito, F. Wypych, J. Mol. Catal. A: Chem. 217 (2004) 121.
[17] M.Z.B. Hussein, Z. Zainal, C.Y. Ming, J. Mater. Sci. Lett. 19 (2000) 879.
[18] J.G. Sharefkin, H. Saltzmann, Org. Synth. 43 (1963) 62.
[19] H.J. Lucas, E.R. Kennedy, M.W. Forno, Org. Synth. 43 (1963) 483.
[20] A. Clearfield, M. Kieke, J. Kwan, J.L. Colon, R.C. Wang, J. Incl. Phenom. Mol. Rec. Chem. 11 (1991) 361.
[21] P. Battioni, J.F. Bartoli, D. Mansuy, Y.S. Byun, T.G. Traylor, J. Chem. Soc. Chem. Commun. 1051 (1991) 0.
[22] M.D. Assis, J.R. Lindsay-Smith, J. Chem. Soc., Perkin Trans. 2 (1998) 2221.
[23] S. Evans, J.R. Lindsay-Smith, J. Chem. Soc., Perkin Trans. 2 (2001) 174.
[24] M.A. Schiavon, Y. Iamamoto, O.R. Nascimento, M.D. Assis, J. Mol. Catal. A: Chem. 174 (2001) 213.
[25] L. Barloy, J.P. Lallier, P. Battioni, D. Mansuy, Y. Pitfard, M. Tournoux, J.B. Valim, W. Jones, New J. Chem. 16 (1992) 71.
[26] A.M. Machado, F. Wypych, S.M. Drechsel, S. Nakagaki, J. Colloid Interface Sci. 254 (2002) 158.
[27] M. Halma, F. Wypych, S.M. Drechsel, S. Nakagaki, J. Porph. Phthal. 6 (2002) 502.
[28] D. Dolphin, T.G. Traylor, L.Y. Xie, Acc. Chem. Res. 30 (1997) 251.